

Published in final edited form as:

Biochemistry. 2011 March 29; 50(12): 2243–2248. doi:10.1021/bi1010514.

Normal Modes of Prion Proteins: From Native to Infectious particle[◇]

Abraham O. Samson^{1,2,‡} and Michael Levitt¹

¹Department of Structural Biology, Stanford University, Stanford, CA 94305, USA

²Faculty of Medicine, Bar-Ilan University, Safed, Israel

Abstract

Prion proteins (PrP) are the infectious agent in transmissible spongiform encephalopathies (i.e. mad cow disease). To be infectious, prion proteins must undergo a conformational change involving a decrease of α -helical content along with an increase of β -strand structure. This conformational change was evaluated by means of elastic normal modes. Elastic normal modes show a diminution of two α -helices by one and two residues, as well as an extension of two β -strands by three residues each which could instigate the conformational change. The conformational change occurs in a region that is compatible with immunological studies, and it is observed more frequently in mutant prions which are prone to conversion, than in WT prions due to differences in their starting structures, which are amplified through normal modes. These findings are valuable for our comprehension of the conversion mechanism associated with the conformational change of prion proteins.

Keywords

Prion proteins; normal modes; conversion mechanism; zipper; dynamics

Prion proteins are the **proteinaceous infectious** particle in neurodegenerative transmissible spongiform encephalopathies (TSE or prion diseases) (1,2). Conversion of cellular PrP (PrP^C) into scrapie PrP (PrP^{Sc}) and aggregation into cytotoxic oligomers is associated with a loss of neuronal cells, resulting in brain spongiosis, which in humans leads to debilitating, dementing and invariably fatal diseases. Examples of TSEs include scrapies in ovines, “mad cow disease” in bovines, as well as Kuru, Creutzfeld-Jacob disease (CJD), fatal familial insomnia (FFI), and Gerstmann-Straussler-Scheinker syndrome (GSS) in humans (3,4).

The prion protein in its native state (PrP^C) is a cell surface receptor anchored to the membrane by a glycosyl phosphatidyl inositol (GPI) at position S230, and carrying two glycosylation sites at N181 and N197 (numbering follows the human species). The PrP^C structure is composed of three helices namely H1 (144–153), H2 (172–192), and H3 (200–225) as well as a small antiparallel β -sheet composed of two β -strands namely S1 (129–130) and S2 (162–163). Its function is not fully understood, but it putatively contributes to transport of copper, neuronal morphology, adhesion, and regulation of lymphocytes (5,6).

[◇]This research was supported by NIH Roadmap for Medical Research PN2 EY016525 and NIH GM41455.

[‡]Corresponding author, Abraham O. Samson, Department of Structural Biology, Stanford University, Stanford, CA 94305, USA, Tel: (650) 725 0754, Fax: (650) 723 8464, avraham.samson@stanford.edu.

Supporting information available. Movies of the normal-mode vibration of the PrP^C (PDB ID 3HAK). This material is available free of charge via the Internet at <http://pubs.acs.org>.

The past decades have seen the extension of our knowledge on prion proteins with the solution of NMR and X-ray structures of various species (7–10) culminating in the elucidation of human prion proteins (11–13). Important advances in relating disease to structure have also been made through the identification of the minimal prion protein fragment that is capable of conferring propagation of the scrapie agent (3). Despite these studies, the transition from PrP^C into PrP^{Sc} remains poorly understood and structures of the monomeric isoforms and oligomers are still unresolved. Fourier-transform infrared (FTIR) spectroscopy and circular dichroism (CD) showed a substantial difference in the secondary structure content between PrP^C and PrP^{Sc}. PrP^C displayed high α -helix content (42%) and little or no β -sheet (3%), while PrP^{Sc} showed high β -sheet content (43%) and a less pronounced α -helix content (30%) (6). These findings suggest that the conversion of α -helices into β -sheets is a fundamental event in the formation of PrP^{Sc} and propagation of prion diseases.

Normal-mode analysis is one of the standard techniques for studying long time dynamics and, in particular, low-frequency motions. In contrast to molecular dynamics, normal-mode analysis provides a very detailed description of the dynamics around a local energy minimum. Even with its limitations, such as the neglect of the solvent effect, the use of harmonic approximation of the potential energy function, and the lack of information about energy barriers and crossing events, normal modes have provided much useful insight into protein dynamics. Over the past years, several techniques have been described to calculate large-scale motions using classical (14–16) and simplified (17–20) normal-mode analysis. Based on these techniques, several executable programs to calculate normal modes have been released, such as ElNemo (21), Nomad-Ref (22) and Normod (unpublished). Similarly, molecular dynamics programs such as GROMACS (23) were modulated to calculate normal modes. Using these programs several molecular dynamics studies have been conducted.

A large number of studies using elastic network models to analyze the molecular dynamics and activity of biological molecules have been carried out (reviewed in (24), (25), (26)). In this study we calculate the normal modes of various prion proteins and assess the conformational transition between PrP^C and PrP^{Sc}. To our knowledge, this is the first attempt to characterize the conformational change of prion proteins using normal modes. We find that normal modes display an increase of β -sheet content alongside a reduction in α -helix content. These findings broaden our understanding of the conformational transition associated with prion protein infection.

Computational procedures

Normal Mode Calculations

To calculate normal modes of the prion proteins, two programs namely Normod (16) and ElNemo (21) were utilized. The normal mode calculations were run locally on a Linux (Ubuntu 8.04) operated desktop computer with a 1.8 GHz Intel Pentium processor and 2GB of RAM. For Normod, normal modes based on realistic force fields (REA) and on elastic network models (TIR) were calculated. For ElNemo, the following default values DQMIN –100, DQMAX 100, DQSTEP 20 were utilized. For both Normod and ElNemo, the 10 non-trivial lowest frequency modes were calculated. For each of these 10 lowest frequency modes, ensembles of 40 PDB files were generated by Normod and 10 PDB files were generated by ElNemo all distorted along the particular mode. The two methods are very different in that Normod (REA) minimizes the structure and then calculates modes in single bond torsion angle space whereas Normod (TIR) and ElNemo avoid minimization by using Tirion elastic motion (17) and a coarse-grained elastic network model (18,19) respectively and then calculate modes in Cartesian coordinate space. Normal modes of the following

prion protein PDB IDs were calculated: 3HAK, 3HAF, 3HEQ, 3HER, and 3HES. If the PDB structures contained a dimer, only one monomer was used.

Secondary structure calculation

To calculate the secondary structure of native structures as well as those distorted along normal modes several programs were utilized. The use of several programs was necessary as not all programs calculate identical secondary structure. The programs which were utilized were Stride (27), DSSP (28) and Encad (29). The consensus secondary structure was considered as that calculated by 2 out of 3 programs.

Secondary structure probability

To calculate the secondary structure probability of prion proteins the program NetSurfP described by Petersen et al. (30) was used.

Modeling of PrP^C isoform and PrP^{Sc}

To construct a model of the PrP^C isoform, the β -sheet of PDB ID 3HAK was elongated to comprise residues 129–163 (S1, S2, and H1). To construct the two models of PrP^{Sc}, the trimeric model postulated by Govaerts et al. (31) was used as a template. The first model is a trimer of the PrP^C isoforms in which the β -sheet are stacked so they can form parallel intermolecular β -sheets. The second model is a trimer of the PrP^C isoforms in which the N-terminus was replaced by a β -helix conformation modeled by Govaerts et al. All models were prepared using Pymol.

Results and Discussion

Normal modes of prion proteins

The normal modes of several prion proteins (3HAK, 3HAF, 3HEQ, 3HER, and 3HES) were calculated. Remarkably, the lowest frequency mode of 3HAK, 3HAF, and 3HER showed an increase in β -structure and decrease in α -structure (Table 1). Other modes also displayed this change, however most often, the first one or two normal modes are enough to describe molecular motions (32) and we decided to focus on the lowest frequency mode.

The conformational change calculated by normal modes corresponds to a 6% increase in β -sheet structure content and a 3% decrease in α -helix content. This conformational change is very small and less pronounced than that observed experimentally (6), and hence the small increase in β -sheet content and decrease in α -helix content should be regarded more like a qualitative tendency. The paper does not claim to have detected a secondary structure change from α -helix to β -sheet (i.e. α -helix turned into β -sheet). The paper claims that there is an overall increase in β -structure and a decrease in α -helix (i.e. random coil changed into β -structure, and α -structure changed into random coil).

The region undergoing the conformational change is consistent with experimental data. Immunological experiments indicated that the major conformational changes which differentiate PrP^C and PrP^{Sc} take place in the N-terminal region (33), since two antibodies targeting the C-terminal helices of PrP^C also recognize PrP^{Sc}. The conformational preservation of these α -helices is also supported by the existence of a disulfide bridge which conjoins them. Therefore, in PrP^C the main conformational change which occurs in the N-terminal region between residues 89 and 172, is in agreement with the region predicted by normal mode dynamics.

The square displacement of C α atoms in the prion proteins which is associated to the lowest frequency mode is shown in figure 1. The C α square displacement values of different prion

structures were scaled to fit in the same graph. Large $C\alpha$ displacements occur in segments with disordered secondary structure while the low motion is observed in secondary structure elements. Nevertheless, the displacement around H1 is high enough to disrupt hydrogen bonds and partially unwind this α -helix. The displacement around the β -strands S1 and S2 allows the elongation of the antiparallel β -sheet.

Prion protein dynamics

A superposition of the ensemble structures of the lowest frequency mode which were generated using Elnemo are shown in figure 2. During this mode, the opposite β -strands S1 and S2 come close, thereby forming new hydrogen bonds which enable the extension of the β -sheet. This increase in β -sheet content is in agreement with experimental data (6).

Normal modes provide a very detailed description of the long term dynamics around a local energy minimum. As such, these data provide a reasonable insight into how spontaneous occurrences of TSE might begin (not end). The conformational transition from the α -helical to the β -rich isoform is separated by a large energetic barrier, yet transformation to prion form seems to occur spontaneously at 10^{-6} to 10^{-7} frequencies during mis- and refolding of yeast proteins (34). For spontaneous occurrence of TSE, spontaneous conversion similar to that instigated during normal modes and involving the β -sheet elongation mechanism is proposed. For transmitted TSE, propagation of prion forms is triggered by interaction of the normal PrP^C with mutant PrP^{Sc}, though it is not clear yet whether the PrP^{Sc} oligomer acts as a seed or the PrP^{Sc} monomer acts as a template for conformational change (34). In any case, the large energetic barrier between the α -helical and β -rich isoforms is lowered and conversions between these two states become more frequent. For both spontaneous and transmitted TSE, the conversion is initiated by zipping together of β -strands S1 and S2. Such “zipping” mechanisms are common in protein structural conversions, and were postulated for polar zippers by Max Perutz (35) and steric zippers of amyloid-like fibrils (36).

In vivo, Prion proteins are glycosylated on residues N181 and N197. These sugar moieties contribute to the stability of the PrP by sterically occluding denaturing interactions (37) without which it would be more prone for conversion. Interestingly, if the sugar moieties were included in the normal mode calculation of the prion protein, then the lowest frequency normal modes showed only bending of the sugar masses and displayed no secondary structure changes (data not shown). This finding is in line with protective role of the carbohydrates observed experimentally. Finally, the long N-terminus of the PrP was not included as there is no structure available at this time.

Previous studies of amyloid fibrils using elastic network modeling studies were reported and showed bending and tensile deformation of the fibrils (38). Also, amyloid nanofibrils display elasticities varying by four orders of magnitude depending on the amino acid sequence (39). These studies on amyloid fibrils however did not have the same intention as the present paper; to our knowledge this is the first attempt to characterize prion protein conformational changes using normal modes.

Propensity for β -structure

Shown in figure 3 is the secondary structure probability for the human prion protein as well as the actual secondary structure of PDB ID 3HAK. The correlation between the β -strand probability and the actual β -sheet is almost perfect. The regions in between the secondary structure elements, in random loop conformation, also correspond to the experimental data. The correlation between helical regions and actual α -helices is a bit less obvious. This could indicate of an easy transition from α -helix to β -strand conformation in the latter region.

Interestingly, elastic network modes of the mutant V129 prions (PDB ID 3HAK, 3HAF, 3HER) showed β -sheet elongation of S1 and S2 while native M129 prions (PDB ID 3HEQ, 3HES) did not (data not shown). Since the motion exhibited by M129 and V129 prions is very similar (figure 1), the diverging final secondary structures are mainly attributed to differences in the starting structures which are amplified through the normal mode motion. For example, the distance between the C α atoms of residues S132 and Q160 which elongate the β -sheet are closer in the V129 prion (4.5 Å in 3HAK), than in the M129 prion (6.0 Å in 3HES). The common methionine/valine polymorphism at residue 129 is a factor that influences prion disease susceptibility. Lee et al. (13) suggested that the disease susceptibility of V129 stems from the inclination of prion proteins to dimerize as seen in crystals of prion proteins containing V129 which revealed both dimeric and monomeric structures. We think that V129 plays an additional role for disease susceptibility as valine has a higher propensity towards β -structure than methionine (40). V129 is located in the center of the first strand (S1) and thus stabilizes the antiparallel β -sheet. The higher propensity for β -sheet which increases the risk of conversion to PrP^{Sc}, works in synergy with the dimerization susceptibility, by lowering the energy barrier to form PrP^{Sc}.

Structure of PrP^{Sc}

To date, there is no published structure of the PrP^{Sc}. The absence of such a structure has made it quite challenging to assess the exact pathway of conversion between PrP^C and PrP^{Sc}. One study suggested that if PrP^{Sc} followed a known protein fold, it would adopt either a parallel β -helical or a β -sandwich architecture in a trimeric assembly (31) (Figure 4). Our normal mode calculations indicative of an elongation of the antiparallel β -sheet into a β -hairpin supports the latter opinion, albeit both are admissible (Figure 4). The β -sandwich could form upon stacking (dimerization) of one β -hairpin of PrP^{Sc} onto another, in line with the idea of steric zippers (36). In figure 4, the lower PrP^{Sc} model oligomerizes by steric stacking of elongated β -sheets (β -sandwich like). Several β -sandwich architectures are available from the SCOP database (41) and without further experimental data it hard to predict the exact PrP^{Sc} structure. Alternatively, the parallel β -helical or β -sandwich architecture could form upon PrP^C dimerization followed by a domain swap mechanism (42). The swap mechanism involves exchange of domains between two proteins (not shown). This working hypothesis is reinforced by the fact that several studies have observed PrP^C dimerization to have an important role in the formation of PrP^{Sc} (13). Prion proteins consist of two main domains, namely S1/H1/S2 and H2/H3. In the lowest frequency mode, these two domains move independently as they have only few interactions (see supplementary information). The independence of the two domains is what enables domain swap more readily. These normal modes data increase our understanding of amyloid formation in TSE of prions.

Conclusion

The mechanism of conformational change which instigates PrP infection was evaluated through normal modes. The normal modes display a decrease of α -helical structure along with an increase of β -structure both occurring in the region involved in PrP conversion through a zipper mechanism. These findings are valuable for our comprehension of the conversion mechanism associated with the conformational change of prion proteins.

Supplementary Material

Refer to Web version on PubMed Central for supplementary material.

Abbreviations

TSE	Transmissible spongiform encephalopathies
PrP	Prion protein
PrP^C	Cellular form of PrP
PrP^{Sc}	Scrapie form of PrP

Acknowledgments

We thank Dr. Dahlia Weiss for careful reading of this manuscript.

References

1. Prusiner SB. Novel proteinaceous infectious particles cause scrapie. *Science*. 1982; 216:136–144. [PubMed: 6801762]
2. Prusiner SB, McKinley MP, Bowman KA, Bolton DC, Bendheim PE, Groth DF, Glenner GG. Scrapie prions aggregate to form amyloid-like birefringent rods. *Cell*. 1983; 35:349–358. [PubMed: 6418385]
3. Jackson GS, Clarke AR. Mammalian prion proteins. *Curr Opin Struct Biol*. 2000; 10:69–74. [PubMed: 10679460]
4. Belay ED. Transmissible spongiform encephalopathies in humans. *Annu Rev Microbiol*. 1999; 53:283–314. [PubMed: 10547693]
5. Isaacs JD, Jackson GS, Altmann DM. The role of the cellular prion protein in the immune system. *Clin Exp Immunol*. 2006; 146:1–8. [PubMed: 16968391]
6. Pan KM, Baldwin M, Nguyen J, Gasset M, Serban A, Groth D, Mehlhorn I, Huang Z, Fletterick RJ, Cohen FE. Conversion of α -helices into β -sheets features in the formation of the scrapie prion proteins. *Proc Natl Acad Sci U S A*. 1993; 90:10962–10966. [PubMed: 7902575]
7. Liu H, Farr-Jones S, Ulyanov NB, Llinas M, Marqusee S, Groth D, Cohen FE, Prusiner SB, James TL. Solution structure of Syrian hamster prion protein rPrP(90–231). *Biochemistry*. 1999; 38:5362–5377. [PubMed: 10220323]
8. James TL, Liu H, Ulyanov NB, Farr-Jones S, Zhang H, Donne DG, Kaneko K, Groth D, Mehlhorn I, Prusiner SB, Cohen FE. Solution structure of a 142-residue recombinant prion protein corresponding to the infectious fragment of the scrapie isoform. *Proc Natl Acad Sci U S A*. 1997; 94:10086–10091. [PubMed: 9294167]
9. Liu H, Spielmann HP, Ulyanov NB, Wemmer DE, James, TL. Interproton distance bounds from 2D NOE intensities: effect of experimental noise and peak integration errors. *J Biomol NMR*. 1995; 6:390–402. [PubMed: 8563467]
10. Calzolari L, Lysek DA, Perez DR, Guntert P, Wuthrich K. Prion protein NMR structures of chickens, turtles, and frogs. *Proc Natl Acad Sci U S A*. 2005; 102:651–655. [PubMed: 15647366]
11. Calzolari L, Lysek DA, Guntert P, von Schroetter C, Riek R, Zahn R, Wuthrich K. NMR structures of three single-residue variants of the human prion protein. *Proc Natl Acad Sci U S A*. 2000; 97:8340–8345. [PubMed: 10900000]
12. Zahn R, Liu A, Luhrs T, Riek R, von Schroetter C, Lopez Garcia F, Billeter M, Calzolari L, Wider G, Wuthrich K. NMR solution structure of the human prion protein. *Proc Natl Acad Sci U S A*. 2000; 97:145–150. [PubMed: 10618385]
13. Lee S, Antony L, Hartmann R, Knaus KJ, Surewicz K, Surewicz WK, Yee VC. Conformational diversity in prion protein variants influences intermolecular beta-sheet formation. *Embo J*. 2010; 29:251–262. [PubMed: 19927125]
14. Brooks B, Karplus M. Harmonic dynamics of proteins: normal modes and fluctuations in bovine pancreatic trypsin inhibitor. *Proc Natl Acad Sci U S A*. 1983; 80:6571–6575. [PubMed: 6579545]
15. Go N, Noguti T, Nishikawa T. Dynamics of a small globular protein in terms of low-frequency vibrational modes. *Proc Natl Acad Sci U S A*. 1983; 80:3696–3700. [PubMed: 6574507]

16. Levitt M, Sander C, Stern PS. Protein normal-mode dynamics: trypsin inhibitor, crambin, ribonuclease and lysozyme. *J Mol Biol.* 1985; 181:423–447. [PubMed: 2580101]
17. Tirion MM. Large Amplitude Elastic Motions in Proteins from a Single-Parameter, Atomic Analysis. *Phys Rev Lett.* 1996; 77:1905–1908. [PubMed: 10063201]
18. Atilgan AR, Durell SR, Jernigan RL, Demirel MC, Keskin O, Bahar I. Anisotropy of fluctuation dynamics of proteins with an elastic network model. *Biophys J.* 2001; 80:505–515. [PubMed: 11159421]
19. Tama F, Sanejouand YH. Conformational change of proteins arising from normal mode calculations. *Protein Eng.* 2001; 14:1–6. [PubMed: 11287673]
20. Delarue M, Sanejouand YH. Simplified normal mode analysis of conformational transitions in DNA-dependent polymerases: the elastic network model. *J Mol Biol.* 2002; 320:1011–1024. [PubMed: 12126621]
21. Suhre K, Sanejouand YH. ElNemo: a normal mode web server for protein movement analysis and the generation of templates for molecular replacement. *Nucleic Acids Res.* 2004; 32:W610–W614. [PubMed: 15215461]
22. Lindahl E, Azuara C, Koehl P, Delarue M. NOMAD-Ref: visualization, deformation and refinement of macromolecular structures based on all-atom normal mode analysis. *Nucleic Acids Res.* 2006; 34:W52–W56. [PubMed: 16845062]
23. Van Der Spoel D, Lindahl E, Hess B, Groenhof G, Mark AE, Berendsen HJ. GROMACS: fast, flexible, and free. *J Comput Chem.* 2005; 26:1701–1718. [PubMed: 16211538]
24. Taly A, Corringer PJ, Grutter T, Prado de Carvalho L, Karplus M, Changeux JP. Implications of the quaternary twist allosteric model for the physiology and pathology of nicotinic acetylcholine receptors. *Proc Natl Acad Sci U S A.* 2006; 103:16965–16970. [PubMed: 17077146]
25. Samson AO, Levitt M. Inhibition mechanism of the acetylcholine receptor by α -neurotoxins as revealed by normal-mode dynamics. *Biochemistry.* 2008; 47:4065–4070. [PubMed: 18327915]
26. Bahar I, Lezon TR, Yang LW, Eyal E. Global dynamics of proteins: bridging between structure and function. *Annu Rev Biophys.* 2010; 39:23–42. [PubMed: 20192781]
27. Frishman D, Argos P. Knowledge-based protein secondary structure assignment. *Proteins.* 1995; 23:566–579. [PubMed: 8749853]
28. Kabsch W, Sander C. Dictionary of protein secondary structure: pattern recognition of hydrogen-bonded and geometrical features. *Biopolymers.* 1983; 22:2577–2637. [PubMed: 6667333]
29. Levitt M. Molecular dynamics of native protein. I. Computer simulation of trajectories. *J Mol Biol.* 1983; 168:595–617. [PubMed: 6193280]
30. Petersen B, Petersen TN, Andersen P, Nielsen M, Lundegaard C. A generic method for assignment of reliability scores applied to solvent accessibility predictions. *BMC Struct Biol.* 2009; 9:51. [PubMed: 19646261]
31. Govaerts C, Wille H, Prusiner SB, Cohen FE. Evidence for assembly of prions with left-handed β -helices into trimers. *Proc Natl Acad Sci U S A.* 2004; 101:8342–8347. [PubMed: 15155909]
32. Krebs WG, Alexandrov V, Wilson CA, Echols N, Yu H, Gerstein M. Normal mode analysis of macromolecular motions in a database framework: developing mode concentration as a useful classifying statistic. *Proteins.* 2002; 48:682–695. [PubMed: 12211036]
33. Peretz D, Williamson RA, Matsunaga Y, Serban H, Pinilla C, Bastidas RB, Rozenshteyn R, James TL, Houghten RA, Cohen FE, Prusiner SB, Burton DR. A conformational transition at the N terminus of the prion protein features in formation of the scrapie isoform. *J Mol Biol.* 1997; 273:614–622. [PubMed: 9356250]
34. Tuite MF, Cox BS. Propagation of yeast prions. *Nat Rev Mol Cell Biol.* 2003; 4:878–890. [PubMed: 14625537]
35. Perutz MF. Glutamine repeats as polar zippers: their role in inherited neurodegenerative disease. *Molecular Medicine.* 1995; 1:718–721.
36. Nelson R, Sawaya MR, Balbirnie M, Madsen AO, Riekel C, Grothe R, Eisenberg D. Structure of the cross- β spine of amyloid-like fibrils. *Nature.* 2005; 435:773–778. [PubMed: 15944695]
37. Rudd PM, Wormald MR, Wing DR, Prusiner SB, Dwek RA. Prion glycoprotein: structure, dynamics, and roles for the sugars. *Biochemistry.* 2001; 40:3759–3766. [PubMed: 11300755]

38. Xu Z, Paparcone R, Buehler MJ. Alzheimer's A β (1–40) amyloid fibrils feature size-dependent mechanical properties. *Biophys J.* 2010; 98:2053–2062. [PubMed: 20483312]
39. Knowles TP, Fitzpatrick AW, Meehan S, Mott HR, Vendruscolo M, Dobson CM, Welland ME. Role of intermolecular forces in defining material properties of protein nanofibrils. *Science.* 2007; 318:1900–1903. [PubMed: 18096801]
40. Chou PY, Fasman GD. Conformational parameters for amino acids in helical, β -sheet, and random coil regions calculated from proteins. *Biochemistry.* 1974; 13:211–222. [PubMed: 4358939]
41. Murzin AG, Brenner SE, Hubbard T, Chothia C. SCOP: a structural classification of proteins database for the investigation of sequences and structures. *J. Mol. Biol.* 1995; 247:536–540. [PubMed: 7723011]
42. Staniforth RA, Giannini S, Higgins LD, Conroy MJ, Hounslow AM, Jerala R, Craven CJ, Waltho JP. Three-dimensional domain swapping in the folded and molten-globule states of cystatins, an amyloid-forming structural superfamily. *Embo J.* 2001; 20:4774–4781. [PubMed: 11532941]

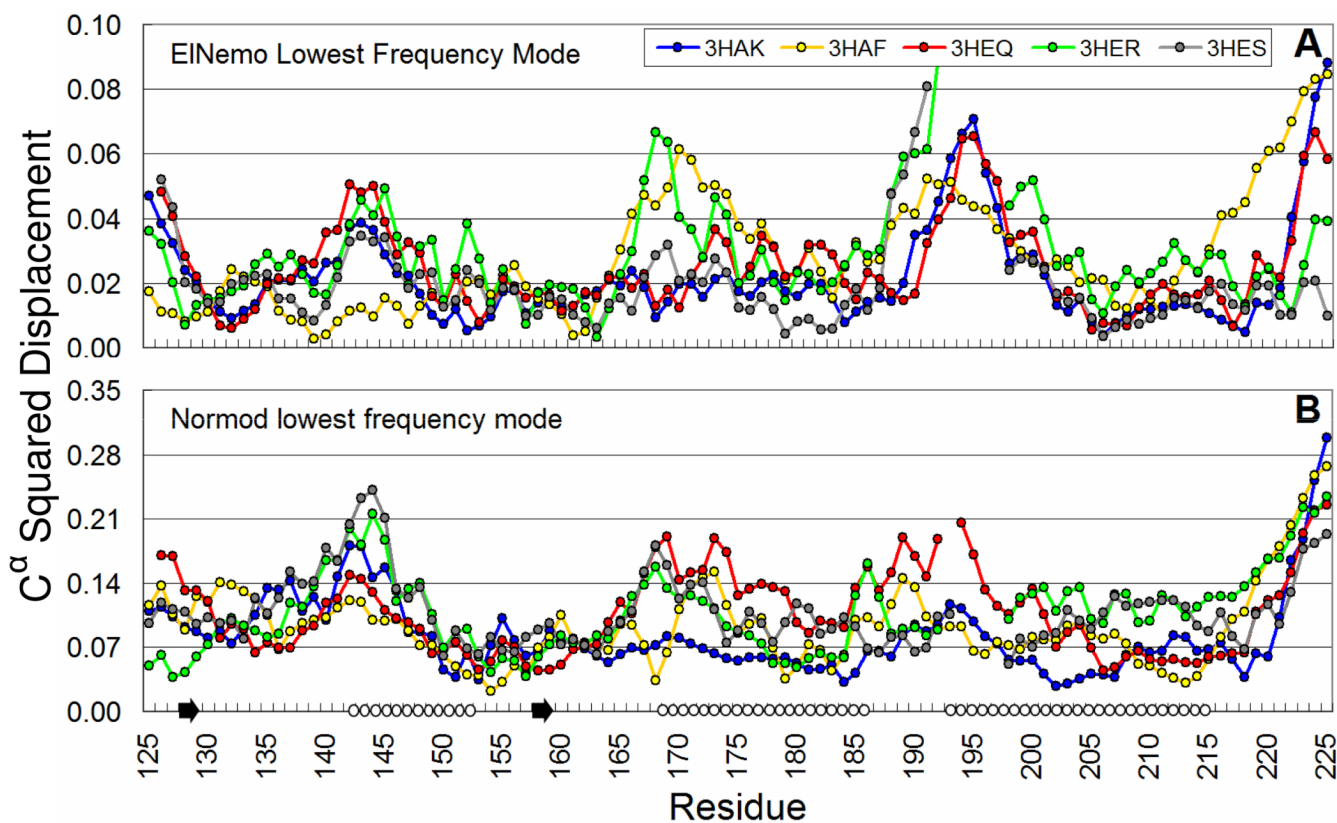


Figure 1. Scaled square displacement of $C\alpha$ atoms of prion proteins

Shown are the scaled $C\alpha$ square displacement values of (A) Elnemo and (B) Normod lowest frequency mode of PDB structures 3HAK, 3HAF, 3HEQ, 3HER, and 3HES. The secondary structure is indicated above the residue axis. Note the minimal displacement around helices and sheets.

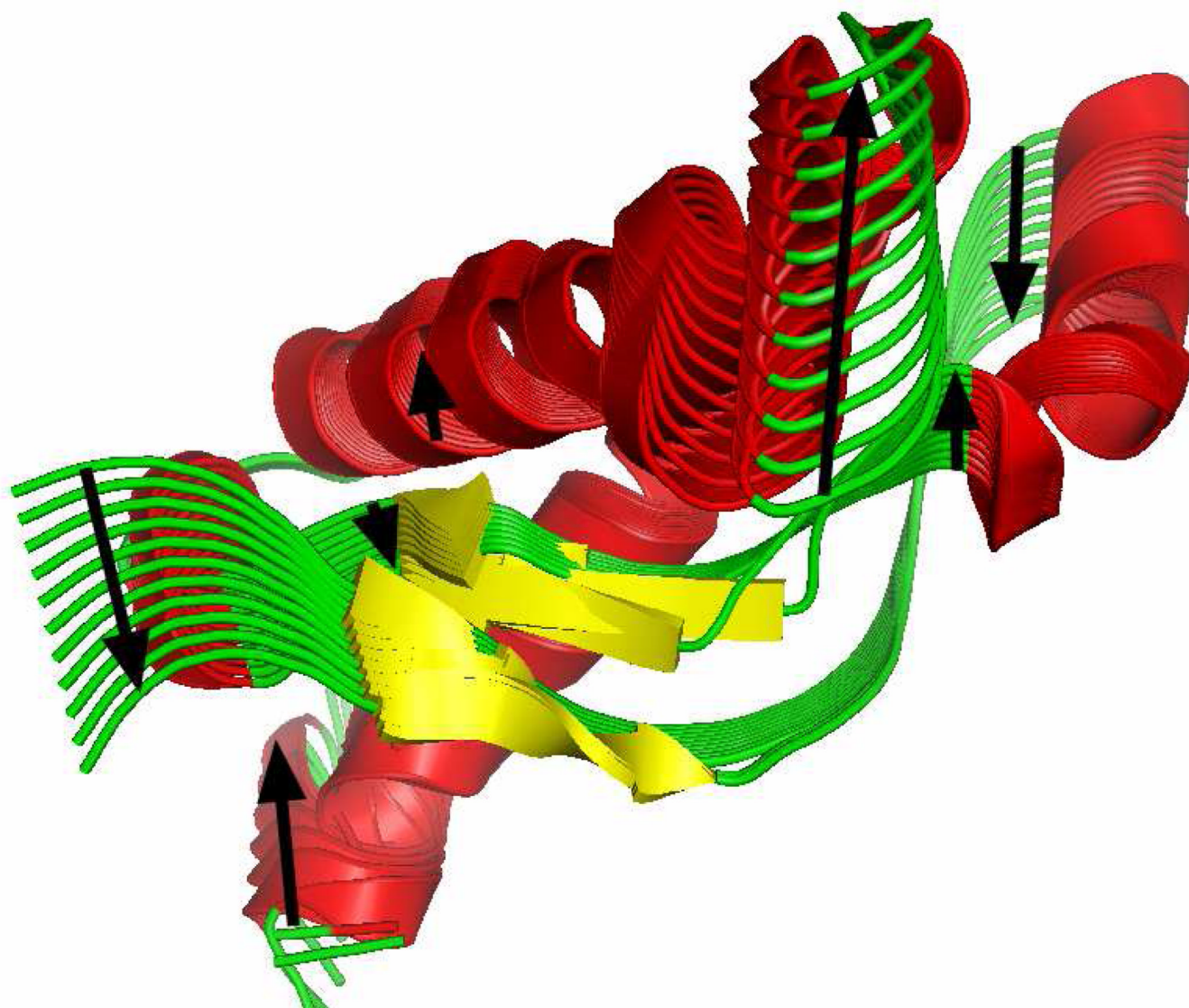


Figure 2. Lowest frequency mode of prion proteins

Shown in cartoon display are the ensemble structures of the lowest frequency mode of E1Nemo of PDB ID 3HAK. Arrows indicate the directions of simultaneous motion in time. Note the elongation of β -strands S1 and S2 (in yellow) which leads to the lengthening of the antiparallel β -sheet“.

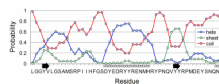


Figure 3. Secondary structure probability of the human M129V mutant prion protein
Shown is the probability for helix, sheet, and coil formation of the M129V mutant prion protein (residues 125–174) calculated using NetSurfP (30). The actual secondary structure of PDB ID 3HAK is indicated above the residue axis.

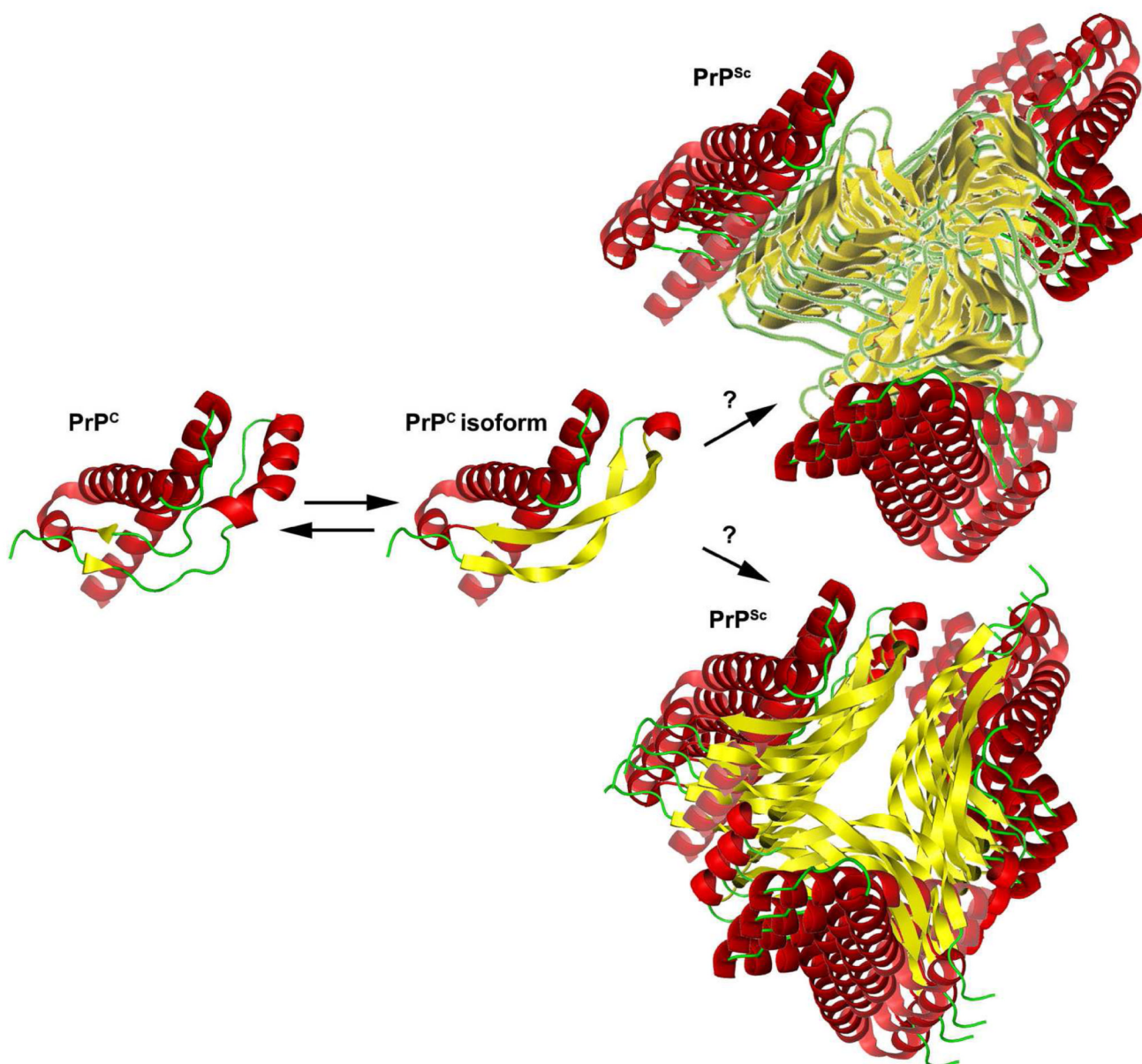


Figure 4. Model of PrP^C isoform and PrP^{Sc}

Shown are cartoon representations of PrP^C structure, putative PrP^C isoform, and two PrP^{Sc} models. The PrP^C corresponds to PDB ID 3HAK. The PrP^C isoform is similar to PrP^C with the exception of a β -sheet elongation. PrP^{Sc} models were based on the trimeric assembly reported by Govaerts et al. (31). In the upper PrP^{Sc}, the N-terminus adopts a β -helix conformation. In the lower PrP^{Sc}, the N-terminus adopts a β -sandwich conformation similar to the steric zipper conformation reported by Nelson et al. (36). The figure was prepared using Pymol.

Table 1

Consensus secondary structure of prion protein (PDB ID 3hak) in the native and normal mode distorted structures.

SEQ 125	•	•	•	•	•	174
Native	LGGYVLGSAMSRPIIHFGSDYEDRYRENMHRYPNQVYYRPMDEYSNQNN					
Distorted	EE	<u>HH</u> HHHHHHHHGGG	EE	GGGGG	HHH	
	EE <u>EEE</u>	HHHHHHHHGGG	<u>EEEE</u>	GGGGG	HHH	
SEQ 175	•	•	•	•	•	224
Native	FVHDCVNIITIKQHTVTTTTKGENFTETDVKMMERVVEQMCITQYERESQA					
Distorted	HHHHHHHHHHHHHHHHHHHH		HHHHHHHHHHHHHHHHHHHHHH <u>H</u>			
	HHHHHHHHHHHHHHHHHHHH		HHHHHHHHHHHHHHHHHHHHHH			